

GT2011-45+)*

DESIGN OPTIMIZATION OF A RETRACTABLE HOLDER FOR COMPRESSOR DISCHARGE BRUSH SEAL

Omprakash Samudralaⁱ
GE Global Research Center
Niskayuna, NY 12309, USA

Christopher E Wolfe
GE Global Research Center
Niskayuna, NY 12309, USA

Siddarth Kumar
Massachusetts Institute of Technology
Cambridge, MA 02139, USA

Raymond E Chupp
GE Energy
Greenville, SC 29615, USA

ABSTRACT

In many industrial gas turbines, a portion of the compressor discharge air is extracted through a secondary flow path to aid the cooling of critical turbine components as well as to supplement purge flow for preventing hot gas ingestion in the first forward turbine bucket wheel space. GE has developed advanced brush seals for controlling the amount of cooling/purge flow passing through this secondary flow path (also called the high pressure packing (HPP) circuit) and has successfully implemented them in the field in a variety of E, F & H class gas turbines. During turbine shutdown, due to a lag in thermal response between the rotor and the stator, interference can result between brush seal bristles and the rotor surface causing significant amounts of wear. This wear can accumulate over several start up / shut down cycles resulting in an increased secondary flow through the HPP circuit and thus a loss in turbine efficiency and power output. In order to alleviate this situation, a seal holder has been designed to passively retract the HPP brush seal, from a low clearance position to a high clearance position, during turbine shut down and thus prevent seal interference/wear.

This paper delves into the design and optimization of a retractable seal. An analytical model was developed to predict the seal motion during startup and shutdown of the turbine. Critical geometry and design parameters affecting seal closure and retraction behavior were identified. In addition, criteria for stability of seal motion were developed and the design was optimized to meet these requirements. Seal wear during turbine shutdown is avoided by ensuring that the seal retracts faster than the rate of thermally induced interference. The effect of design variables was minimized to ensure seal closure and retraction behavior does not vary significantly over the

operating life of the seal. Model predictions were validated by subscale rig tests performed in the laboratory.

NOMENCLATURE

Δp = Pressure differential across the seal

$a = W_{BP} + xW_{ST}$, Length governing radial pressure force

W_{BP} = Back plate width

W_{ST} = Bristle pack axial width

x = Fraction based on how the pressure changes under the bristle pack
0.5 for linear variation, < 0.5 for nonlinear variation

$\underline{a} = \frac{a - a_{\min}}{a_{\max} - a_{\min}}$, normalized a

$b = H_{ST} - yH_{SH}$, Length governing axial pressure force

H_{ST} = Seal height

H_{SH} = Support hook height

y = Fraction based on how the pressure changes at the gas joint
0.5 for linear variation

$\underline{b} = (b - b_{\min}) / (b_{\max} - b_{\min})$, normalized b

L = Segment length (straight)

L_c = Segment length (curved)

μ = Coefficient of friction

μ_{st} = Static coefficient of friction

μ_{dyn} = Dynamic coefficient of friction

N_s = # of leaf springs

K_s = Spring stiffness

$\underline{K}_s = K_s / K_s^{nom}$, normalized spring stiffness

δ = Seal motion (Spring deflection)

δ_{max} = Maximum possible seal motion (Max spring deflection)

δ_{wt} = Deflection due to seal weight

δ_{pre} = Deflection due to preload

$\hat{\delta} = \frac{\delta}{\delta_{max}}$ = Normalized seal displacement

Δp_{max} = Max seal pressure differential (steady state condition)

$\Delta \hat{p} = \frac{\Delta p}{\Delta p_{max}}$ = Normalized seal pressure differential

ϕ = Segment angular position (deg) from the top dead center (TDC).

$\phi = 180^\circ$ for bottom dead center

$\hat{\delta}_{wt} = \delta_{wt} \cos \phi$

= Deflection due to weight for segments not at TDC

Wt = Weight of the seal segment

$\hat{W}t = Wt \cos \phi$

= Effective weight for segments not at TDC

INTRODUCTION

In many large frame industrial gas turbine designs, a portion of the compressor discharge air is diverted/extracted via a cooling circuit (secondary flow path) to aid in the cooling of the rotor, critical turbine components as well as to supplement purge flow for preventing hot gas ingestion into the first forward turbine bucket wheel space (Wolfe et. al. [1]). GE has developed advanced brush seals for controlling the amount of cooling/purge flow passing through this secondary flow path (hence forth called the high pressure packing (HPP) circuit) and has successfully implemented them in the field in a variety of E & F class gas turbines (Dinc & Turnquist [2], Bagepalli et. al. [3], Aksit et. al. [4], Chupp et. al. [5], Dinc et. al. [6]). The cross section of a typical industrial gas turbine is shown in Figure 1 and the location of the high-pressure packing seal is indicated therein. The high-pressure packing seal (see Figure 2) maintains a tight control over the amount of cooling/purge flow through the HPP circuit to minimize loss in overall turbine efficiency and power output due to compressor extraction.

Conventional brush seals offer many advantages compared to traditional labyrinth seals and as such are increasingly being used in industrial gas turbines. They are contact seals, with the bristles riding on the rotor allowing for near-zero clearance between the rotor & stator. In addition, bristle flexibility allows them to accommodate eccentricity in rotor motion as well as

relative radial movement between rotor/stator without loss of contact with the rotor. They can also compensate for small clearances using the “blow-down effect”, which allows the bristles to move radially inward and make contact with the rotor in the presence of a pressure differential across it. They are easy to assemble – can be assembled with interference - with the bristles eventually wearing down to the correct size. However, they cannot handle transients (start-up /shut-down / hot restart etc.) that can result in large interferences between the rotor and stator. Excessive bristle-wear can occur (that cannot be compensated by the blow-down effect) eventually resulting in increased steady state leakage. A brush seal mounted on a retractable seal holder, which can move the seal away from the rotor during such transient events, will avoid the degradation in leakage performance thereby sustaining the benefits of a brush seal for the life of the seal.

During turbine shutdown, the lag in thermal response between the rotor and the stator at the high-pressure packing brush seal location results in significant interference (“shut down pinch”) followed by possible wear of the bristles (Aksit & Tichy [7]). Figure 3 shows a worn brush seal after its operating life showing the degradation in fence height, which was initially larger than the thickness of the back plate. Figure 4 shows the typical axial and radial transients experienced during shutdown of a gas turbine. As shown in the graph, the seal clearance turns negative (interference), which can result in significant wear. This wear can accumulate, resulting in a permanent increase in secondary flow through the HPP circuit (during steady state operation) and loss in turbine efficiency and power output.

In order to alleviate this problem, a passively actuated seal holder has been designed to retract the HPP brush seal, from a low clearance position to a high clearance position, during turbine shut down and thus prevent rotor/bristle interference and wear. The retraction is accomplished passively by means of leaf springs, which respond to the change in pressure drop across the seal during the shutdown process. The operating principle of a retractable seal is shown in Figure 5. The principle is the same irrespective of the type of seal being retracted - a brush seal, one or more labyrinth teeth or a combination of both. Hence, the treatment from now on is equally applicable to any of these combinations. Similar retraction technology has been successfully implemented in GE steam turbines for moving packing rings radially to avoid interference during start up / shut down transient events (Dinc et. al [8], O’clair et. al. [9], Chevrette & Bailey [10]).

Alternately, an active retractable seal system can also be used to deal with the shut down “pinch”. One such system incorporating pneumatic actuators was developed by GE and demonstrated in the field. A passive system like the one described here can offer higher reliability and lower cost (compared to an active system) making it a very attractive option for combating the shut down “pinch”.

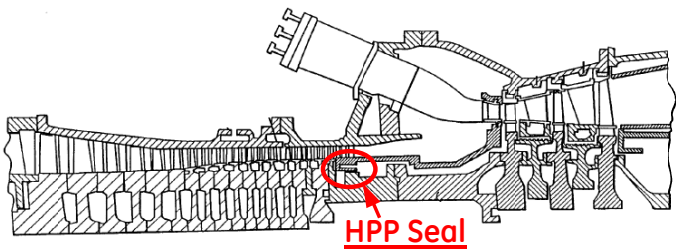


Figure 1 Typical cross section of an industrial gas turbine indicating the position of the High Pressure Packing seal.

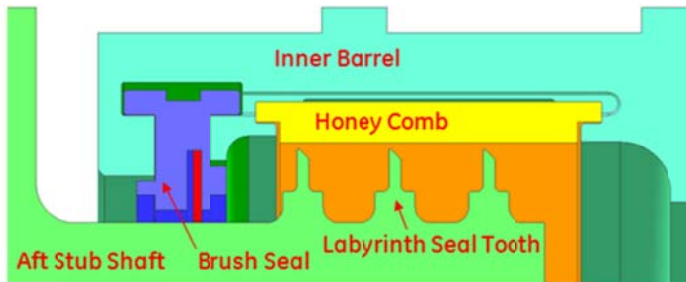


Figure 2 HPP seal in a GE E-class gas turbine showing a brush seal and honeycomb labyrinth seal arranged in series.

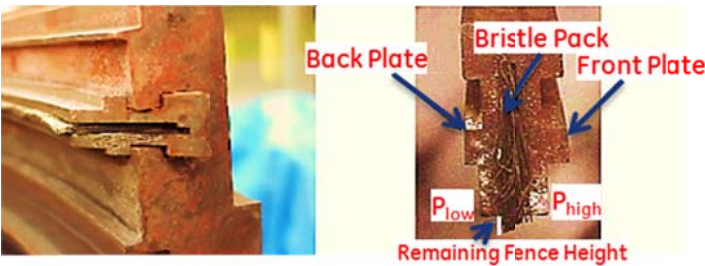


Figure 3 Worn brush seal after 24000 hours of operation.

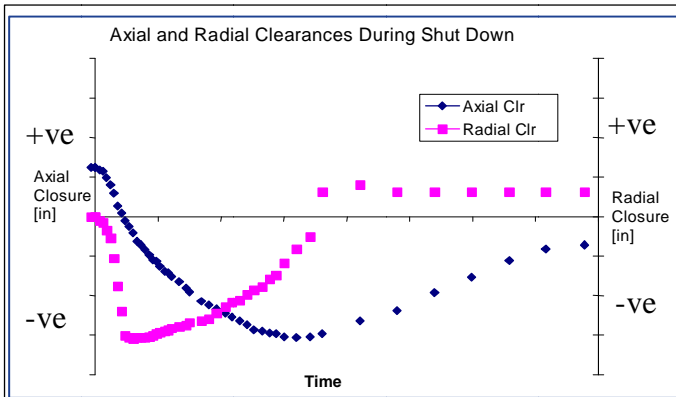


Figure 4 Axial and Radial Clearances at HPP Seal Location during Turbine Shutdown.

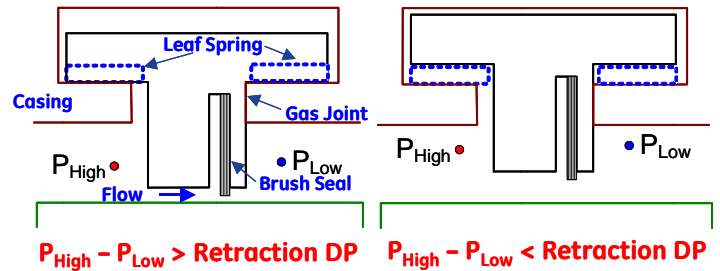


Figure 5 Schematic showing the operation of a retractable seal.

SEAL CONFIGURATION

A regular brush seal is rigidly fixed in its mating slot on the stator. A retractable brush seal, on the other hand, enjoys a degree of freedom allowing it to move radially in and out a finite distance towards and away from the rotor. This is achieved by mounting leaf springs (see Figure 6) between the brush seal and its mating slot, which deflect a finite amount in response to the pressure differential across the seal. The maximum spring deflection possible (before the seal wings make contact with the support hooks) determines the net radial motion of the seal. For this particular design, passive actuation is provided by means of leaf springs (per segment) positioned in slots cut into the outer seal wings (see Figure 6, Figure 7). The retractable seal is mounted on the stator support hooks in a high clearance position (relative to the rotor), with the leaf springs compressed slightly resulting in a preload on the springs.

During turbine startup, extraction flow from the compressor begins to flow through the HPP circuit resulting in a pressure drop across the seal. Once the pressure drop exceeds a design threshold, the retractable seal moves from its initial high clearance position to a low clearance position (usually line-on-line condition) with respect to the rotor. The exact nature of seal closure from the high clearance position to the low clearance position is dependent on the seal/mating slot geometry, friction characteristics of the seal/support hook contact surface and the actuator stiffness. It is desirable that this seal closure begins during the early stages of the turbine start up process and is completed by the time steady state condition is achieved (full load or part load).

During turbine shutdown, the pressure drop across the seal drops monotonically and when it falls below another design threshold, the leaf springs will rebound, causing the seal to move away from the rotor, i.e., from a low clearance position to a high clearance position. It is desirable that the seal retraction begin as early as possible during the turbine shutdown process so as to minimize thermal interference (and consequent bristle wear) and that the retraction occur at a faster rate as compared

to the rate of thermally induced interference between the rotor and stator.

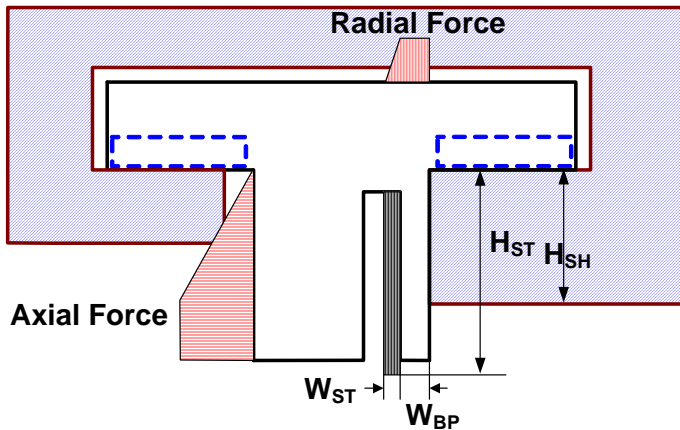


Figure 6 Cross section of a retractable brush seal showing the axial and radial pressure forces and key geometry parameters.

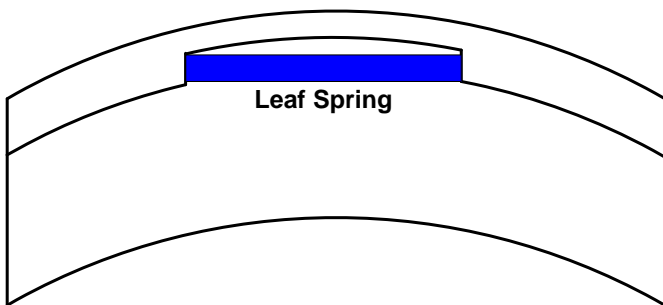


Figure 7 Axial view of a retractable seal segment showing the leaf spring.

The cross-section of a retractable brush seal segment tested in our laboratory is shown in Figure 6. The flow is from left to right, which results in a pressure drop across the seal and net axial and radial pressure forces as shown in Figure 6. Apart from the sealing between the bristles and the rotor, the net axial force also results in a tight seal at the contact surface between the seal and the right support hook (gas joint), thus preventing leakage through the gap between the seal and the mating slot. The seal is initially assembled in a high clearance position with a slight preload on the springs. The preload can be achieved by adding wings at the bottom of the seal or by adding a third leaf spring between the seal and the roof of the mating slot. A schematic of the various forces acting on the retractable brush seal during seal closure and retraction is shown in Figure 8. Note that during retraction the direction of the gas joint friction forces is reversed as compared to the closure event.

In a gas turbine, the closure/retraction behavior of the brush seal segment varies slightly based on the position of the seal segment along the stator groove. For instance, the retraction of

the segment at the top dead center is opposed by the segment weight, whereas the retraction of the segment at the bottom dead center is supported by the segment weight. To ensure all segments close and retract “simultaneously” the effect of segment weight must be small compared to the pressure forces & the spring forces. For the particular design examined in the paper, the segment weight is up to two orders of magnitude smaller than the radial pressure force (during closure/retraction). In addition, for the actual field design, features added at the intersegment gap ensure all segments move simultaneously inward and outward from the rotor at an average pressure differential.

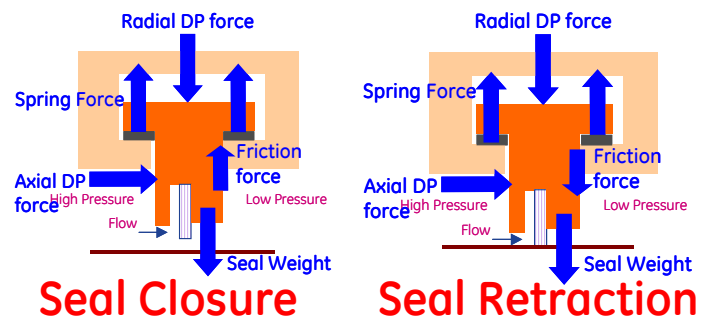


Figure 8 Forces acting on the retractable brush seal during closure and retraction.

RETRACTABLE SEAL – OPERATIONAL REQUIREMENTS

The key operational requirements of a retractable seal are:

1. Seal closure (during turbine start up) must begin only after the pressure differential across the seal exceeds a design threshold.
2. Seal closure must be complete before the pressure differential exceeds that associated with the lowest possible steady state operating load on the turbine.
3. Seal closure behavior must meet criterion 1 & 2 for all possible variations in static & dynamic friction coefficients at the seal/support hook contact face over the life of the seal. The friction coefficients can change appreciably over the seal life (48000 hrs) due to possible corrosion, oxidation, surface wear etc.
4. Seal retraction (during turbine shutdown) must begin soon after the pressure differential across the seal drops below a design threshold.
5. Seal retraction must proceed at a rate faster than the rate at which clearance reduction occurs (due to thermally induced interference) during shut down.
6. Seal retraction behavior must meet criterion 4 & 5 for all possible variations in static & dynamic friction coefficients at the seal/support hook contact face over the life of the seal.

SEAL CLOSURE MODEL

The net radial force acting on the retractable seal during turbine start up (seal in high clearance position) is given by

$$F_{radial}^{closure} = \Delta p [aL - \mu L_c \{b - (\delta_{max} - \hat{\delta}_{wt} - \delta_{pre})\}] - N_s k_s \delta_{pre}$$

Seal closure begins when the net radial force turns positive after overcoming the static friction at the gas joint and the spring resistance. The pressure differential across the seal when seal closure initiates is given by

$$\Delta p_{closure}^{init} = \frac{N_s k_s \delta_{pre}}{aL - \mu_{static} L_c \{b - (\delta_{max} - \hat{\delta}_{wt} - \delta_{pre})\}}$$

As seen from the above equation, there exists a threshold on the static friction coefficient at the gas joint, beyond which the seal will never close. This maximum allowable static friction coefficient at the gas joint is given by

$$\mu_{static} < \frac{aL}{L_c \{b - (\delta_{max} - \hat{\delta}_{wt} - \delta_{pre})\}}$$

The above relation places limits on the rates at which radial and axial forces acting on the seal can increase with pressure differential. By choosing appropriate values for the two length parameters a and b , as well as an appropriate preload, δ_{pre} , the above relation can be satisfied at all possible static friction coefficients at the gas joint expected during the life of the seal. Figure 9 is a contour plot showing the maximum allowable static friction coefficient at the gas joint for all possible seal length parameters a and b (normalized). The retractable seal segment considered here was a 300 mm (12 in) long segment tested in the laboratory with a 1320 mm (52 in) diameter rotor. The seal cross section was the same as one of the GE gas turbine brush seals currently operational in the field. A preload of 0.127 mm (5 mil) was assumed. Figure 9 can be used to choose the seal length parameters based on the expected static friction coefficients at the gas joint over the operating life of the seal. Note that the length parameter a governs the thickness of the back plate and the length parameter b governs the height of the downstream support hook.

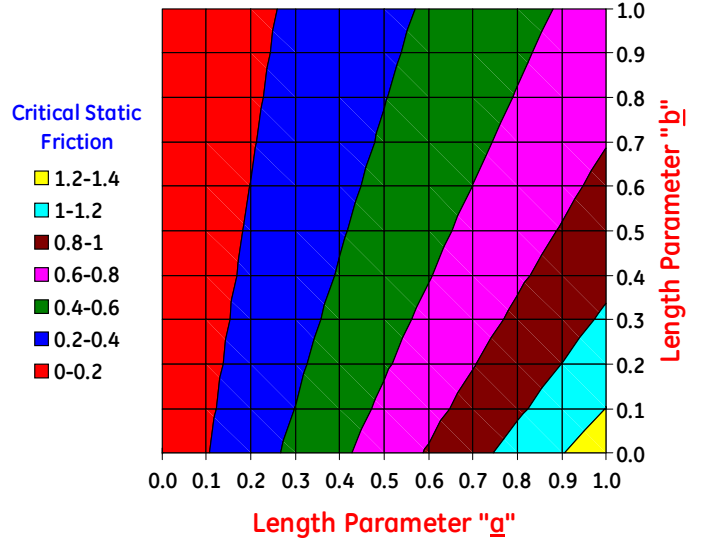


Figure 9 Maximum allowable static friction coefficient at the gas joint for different normalized seal length parameters.

Once the seal closure initiates, a net positive radial force (inward) is generated due to the friction at the gas joint changing from a higher static value to a lower sliding value. This radial force causes the seal to move closer to the rotor by an amount given by

$$\delta_1 = \frac{\Delta p_{closure}^{init} [aL - \mu_{dynamic} L_c \{b - (\delta_{max} - \hat{\delta}_{wt} - \delta_{pre})\}] - N_s k_s \delta_{pre}}{\Delta p_{closure}^{init} \mu_{dynamic} L_c + N_s k_s}$$

The seal closure may or may not be completed in one step. In such a case, the seal pauses at an intermediate position and waits for the pressure differential to increase to a higher value before it resumes motion. Thus seal closure is accomplished in a stick-slip type of motion. The amount the seal moves towards the rotor in each step depends on the radial force generated due to the static friction changing to dynamic friction at the gas joint and the resistance offered by the springs. The seal pressure differential and the net seal motion at the n th step are given by

$$\Delta p_{closure}^n = \frac{N_s k_s (\delta_{pre} + \delta_{n-1})}{aL - \mu_{static} L_c \{b - (\delta_{max} - \hat{\delta}_{wt} - \delta_{pre} - \delta_{n-1})\}}$$

$$\delta_n = \frac{\Delta p_{closure}^n [aL - \mu_{dynamic} L_c \{b - (\delta_{max} - \hat{\delta}_{wt} - \delta_{pre})\}] - N_s k_s \delta_{pre}}{\Delta p_{closure}^n \mu_{dynamic} L_c + N_s k_s}$$

Seal closure is complete when the seal reaches its lowest clearance position

$$\delta_n \geq \delta_{\max} - \hat{\delta}_{wt} - \delta_{pre}$$

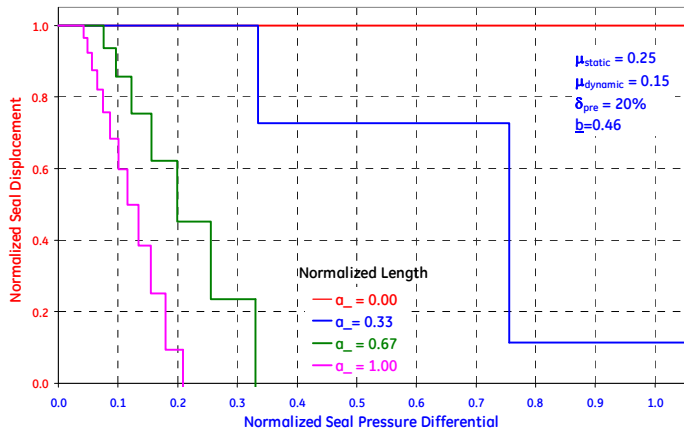


Figure 10 Seal closure curves for $\mu_{st} = 0.25$, $\mu_{dyn} = 0.15$.

Figures 10, 11 and 12 show seal closure curves – seal motion from high clearance position to low clearance position as a function of the seal pressure differential. Figure 10 shows the curves for nominal values of the static friction coefficient (0.25) and dynamic friction coefficient (0.15). It can be readily seen that for large values of the normalized length parameter a (implies high radial pressure forces), seal closure can be very sharp, occurring within a few psi change in seal pressure differential. On the other hand, small values of a , can result in seal closing too late or not closing at all.

Figure 11 shows the seal closure curves for very low values of gas joint static and dynamic friction coefficients, 0.05 and 0.0 respectively. As can be readily seen, the effect of length parameter b is negligible with all the curves almost falling on top of each other. The parameter b drives the net axial pressure force acting on the seal (and thus the gas joint friction force). For small values of friction coefficients, it becomes negligible making the closure curves insensitive to b .

Figure 12 shows the seal closure curves for a case with a large variation in static and dynamic friction coefficients, 0.5 and 0.1 respectively. In such a case, for appropriate values of the length parameters, a and b , seal closure may be accomplished in one or two steps. The large difference between static and dynamic friction coefficients leads to a large net radial closing force, which can result in complete seal closure in only a step or two.

Figure 13 shows a contour plot of the seal pressure differential at which closure initiates for a whole range of possible static and dynamic friction coefficients. For the chosen values of seal geometry, preload and spring stiffness, this plot indicates that

the seal closure will begin within a few psi for the entire possible range of friction coefficients. Note that dynamic friction coefficient is always smaller than the static friction coefficient and hence the area in top left is not feasible. Figure 14 shows the pressure differential at which seal closure is complete for the entire range of possible gas joint friction coefficients. It provides a map of the variation in seal closure completion DP as the friction coefficients change during the life of the seal.

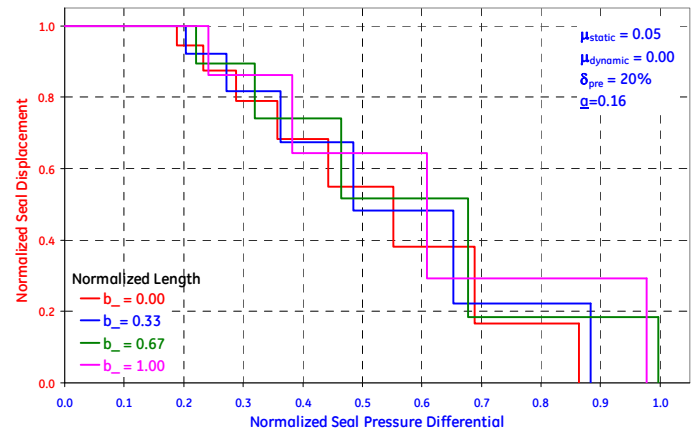


Figure 11 Seal closure curves for $\mu_{st} = 0.05$, $\mu_{dyn} = 0.0$.

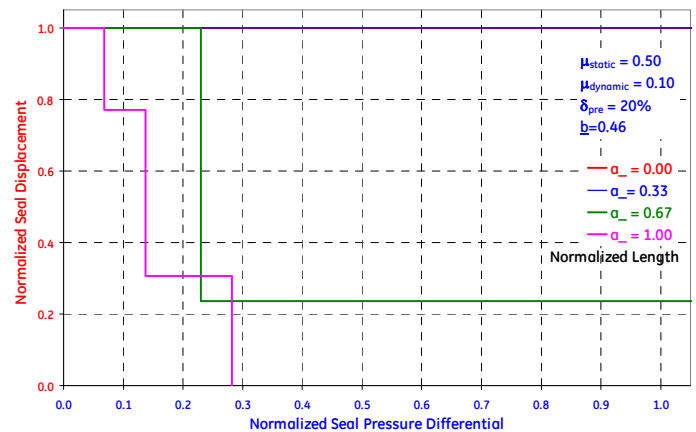


Figure 12 Seal Closure curves for $\mu_{st} = 0.5$, $\mu_{dyn} = 0.1$.

Figure 15 shows the effect of spring stiffness on the seal closure behavior. As can be readily expected, higher spring stiffness leads to the seal closure beginning at a later point during the turbine startup process and also ending at a later point during the startup process. Figure 16 shows the effect of preload on the seal closure behavior. Higher preload results in seal closure beginning later during the startup process, but the closure process remains approximately the same.

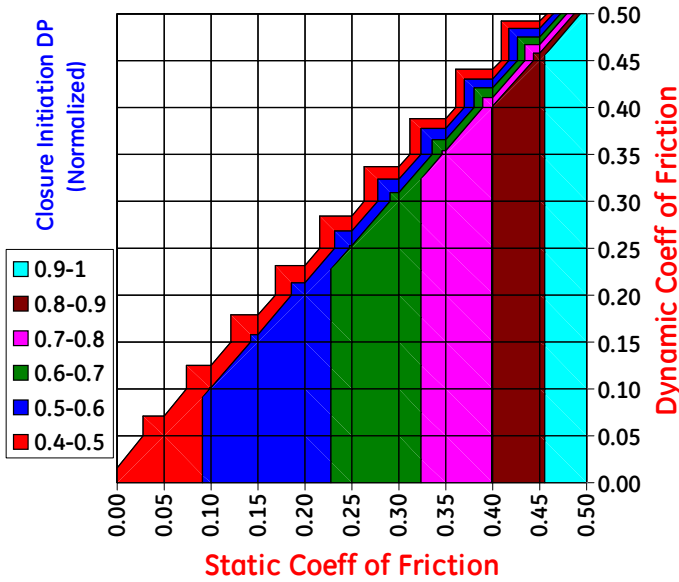


Figure 13 Contour plot showing the seal closure initiation DP for all possible friction coefficients over the life of the seal.

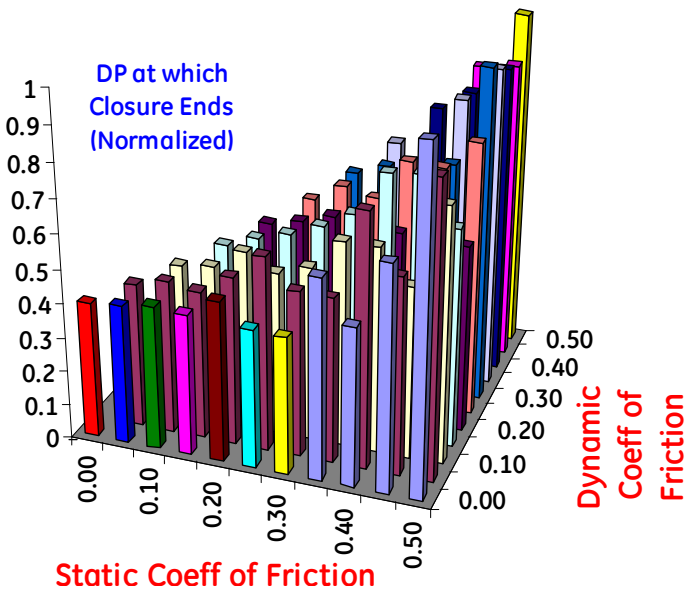


Figure 14 Plot showing the DP at which seal closure is complete for all possible friction coefficients over the life of the seal.

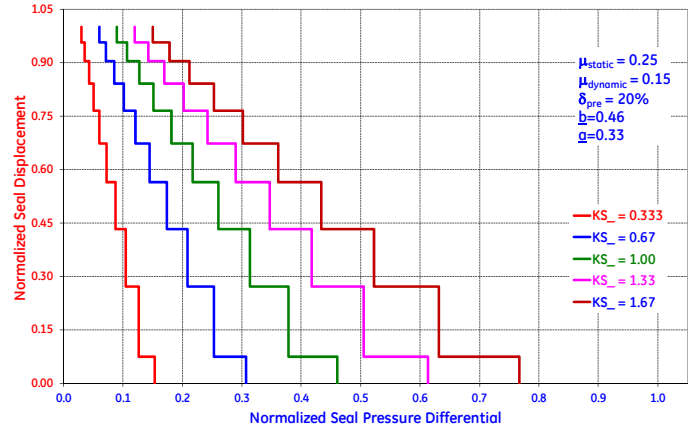


Figure 15 Effect of spring stiffness on seal closure behavior.

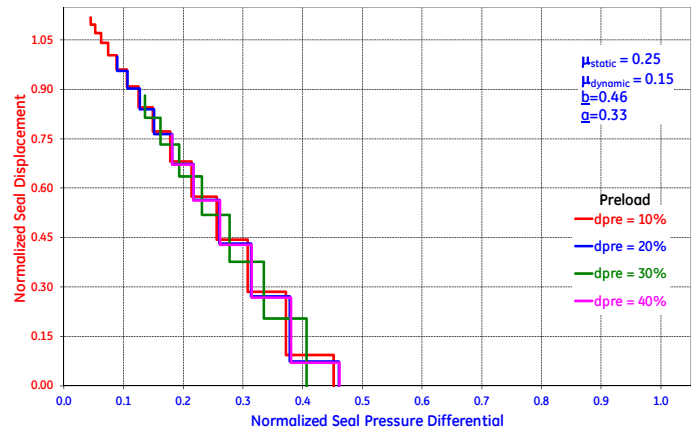


Figure 16 Effect of preload on seal closure behavior.

SEAL RETRACTION MODEL

The net radial force acting on the retractable seal during turbine shut down (seal in low clearance position) is given by

$$F_{radial}^{retract} = N_s k_s \delta_{max} - \hat{W}t - \Delta p [aL + \mu L_c b]$$

Seal retraction begins when the net radial force (outward) turns positive after overcoming the static friction at the gas joint, the radial pressure force and the seal weight. The pressure differential across the seal when seal retraction initiates is given by

$$\Delta p_{retract}^{init} = \frac{N_s k_s \delta_{max} - \hat{W}t}{aL + \mu_{static} L_c b}$$

Unlike seal closure, there is no threshold on the static friction coefficient for retraction. Seal will always retract before the

turbine shut down is complete. The amount of retraction in the first step is given by

$$\delta_1 = \frac{\Delta p_{retract}^{init} L_c b (\mu_{static} - \mu_{dynamic})}{N_s k_s - \Delta p_{retract}^{init} \mu_{dynamic} L_c}$$

Similar to seal closure, seal retraction may or may not be completed in one step. The seal pressure differential and the net seal motion at the nth retraction step are given by

$$\Delta p_{retract}^n = \frac{N_s k_s (\delta_{max} - \delta_{n-1}) - \hat{W}t}{aL + \mu_{static} L_c (b - \delta_{n-1})}$$

$$\delta_n = \frac{N_s k_s \delta_{max} - \hat{W}t - \Delta p_{retract}^n [aL + \mu_{dynamic} L_c b]}{N_s k_s - \Delta p_{retract}^n \mu_{dynamic} L_c}$$

Seal retraction proceeds until the seal reaches its high clearance position.

$$\delta_n \geq \delta_{max} - \hat{\delta}_{wt} - \delta_{pre}$$

Figures 17, 18 and 19 show seal retraction curves – seal motion from low clearance position to high clearance position as a function of the seal pressure differential. Figure 17 shows the curves for nominal values of the static friction coefficient (0.25) and dynamic friction coefficient (0.15). It can be readily seen that for large values of the normalized length parameter a (implies high radial pressure forces), seal retraction will occur late in the shut down process, but the retraction rate will be fast. On the other hand, small values of a , can result in seal retraction to start early, but the retraction rate will be slower.

Figure 18 shows the seal retraction curves for very low values of gas joint static and dynamic friction coefficients, 0.05 and 0.0 respectively. As can be readily seen, the effect of length parameter b is negligible with all the curves falling on top of each other. This is due to the low gas joint friction forces arising from small friction coefficients.

Figure 19 shows the seal retraction curves for a case with a large variation in static and dynamic friction coefficients, 0.5 and 0.1 respectively. In such a case, for appropriate values of the length parameters, a and b , seal closure may be accomplished in one or two steps. The large difference between static and dynamic friction coefficients leads to a large net radial opening force, which can result in complete seal closure in only a step or two.

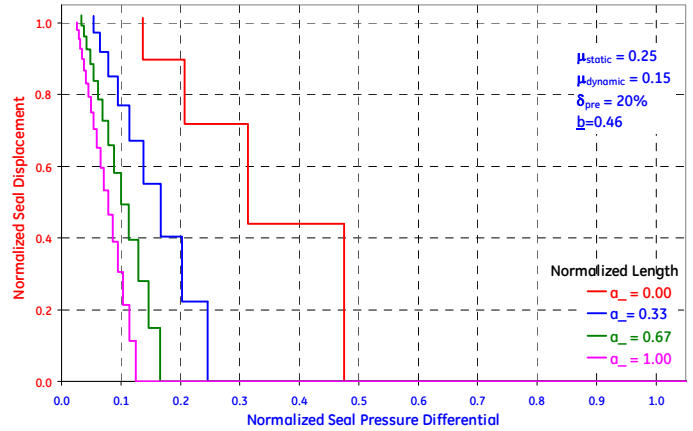


Figure 17 Seal Retraction Curves for $\mu_{st} = 0.25$, $\mu_{dyn} = 0.15$.

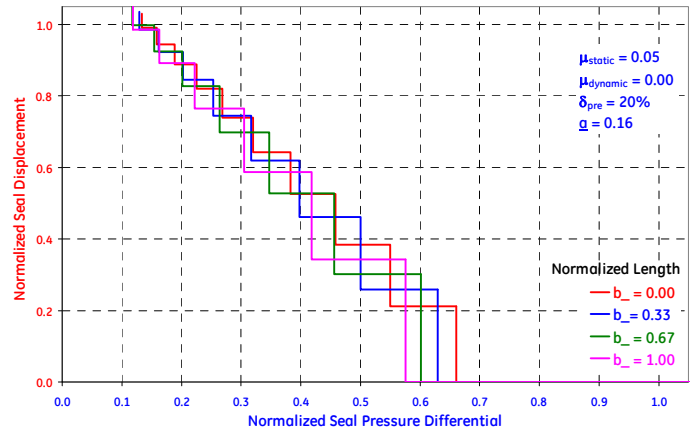


Figure 18 Seal Retraction Curves for $\mu_{st} = 0.05$, $\mu_{dyn} = 0$.

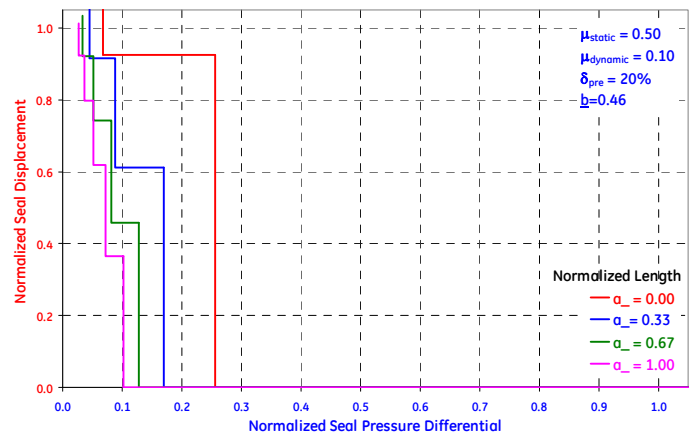


Figure 19 Seal Retraction Curves for $\mu_{st} = 0.5$, $\mu_{dyn} = 0.1$.

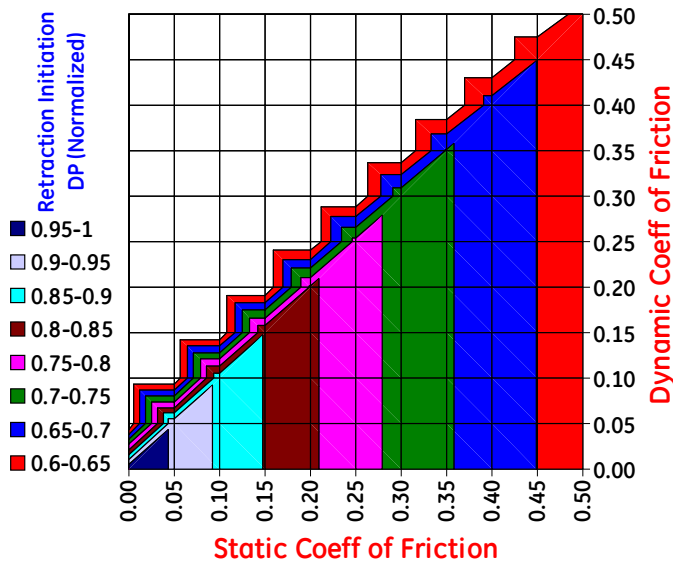


Figure 20 Contour plot showing the seal retraction initiation DP for a range of friction coefficients.

Figure 20 shows a contour plot of the seal pressure differential at which retraction initiates for a whole range of possible static and dynamic friction coefficients. For the chosen values of seal geometry, preload and spring stiffness, this plot indicates that the seal retraction will begin within a small DP range for all possible friction coefficients. Note that dynamic friction coefficient is always smaller than the static friction coefficient and hence the area in top left is not feasible. For finite spring stiffness, retraction is guaranteed before the turbine shut down is complete.

Spring stiffness plays a significant role in the seal retraction behavior. Higher spring stiffness leads to seal retraction occurring later in the shutdown process. However, retraction occurs at a faster rate. Optimal spring stiffness must be chosen to ensure that retraction begins before significant rotor/seal interference occurs and also to ensure that the retraction rate is faster than the interference rate. Spring preload has no effect on seal retraction behavior.

By choosing appropriate values of the normalized length parameters a and b , preload δ_{pre} and spring stiffness the desired closure & retraction characteristics can be achieved. Closure/retraction curves and closure/retraction maps (as shown above) aid in ensuring that the design selected is optimal or close to optimal and meets the operational requirements of the seal. It must be understood that the closure/retraction model predictions are conservative. For instance, at each step of the closure/retraction process it is assumed that the friction coefficient climbs back to its static value. Most likely scenario would be the friction coefficient rising only to an intermediate value. Vibrations will also prevent the seal from achieving perfect contact at each intermediate step in the closure/retraction process. In such a case, seal closure/retraction

may be more gradual and not stick-slip like as the models predict.

STABILITY OF SEAL MOTION

A retractable seal must maintain its attitude with respect to its mating slot during the radial motion from high clearance position to low clearance position and vice versa. If the attitude of the retractable brush seal during seal motion is such that the plane of the bristle pack remains perpendicular to the rotor axis, it is said to be stable. On the other hand, if the seal rotates causing the bristle pack to move away from a plane perpendicular to the rotor axis, it is said to be unstable.

The stability of a retractable seal can be checked in the following manner

- A rigid body rotational motion is assumed at all seal positions during closure and retraction processes.
- The axis of rotation for such motion is determined.
- The total moment about this axis, caused by the pressure forces, friction forces, spring forces and seal weight is calculated.
- If the total moment about the clockwise rotation center is clockwise (at any point in seal motion), then the seal is unstable and will rotate instead of moving in a purely radial manner. On the other hand, if the total moment about the clockwise rotation center is counter-clockwise, then the seal motion is stable.
- If the total moment about the counter-clockwise rotation center is counter-clockwise (at any point in seal motion), then the seal is unstable and will rotate instead of moving in a purely radial manner. On the other hand, if the total moment about the counter-clockwise rotation center is clockwise, then the seal motion is stable.

It is not possible to derive closed form expressions for all the moments acting on the seal, especially when pressure variations are non-linear (e.g., under the bristle pack) (see Chen et. al. [11]). Software codes have been developed incorporating numerical integration techniques to determine if a particular seal design is stable at each point in the seal motion.

Figure 21 shows a retractable seal in its lowest clearance position. Once the turbine is shut down, the seal can either move radially away from the rotor or rotate (CW or CCW) about its axis of rotation. For CCW rotation, the seal remains in contact with the points G & H on the extremities of the support hook as well as the point P on the seal mating slot. Note that the seal contact points at G & H move radially outward, whereas the contact point at P moves axially inward. This results in an axis of rotation parallel to the straight line joining G & H and radially beneath the point P (see Figure 21).

As seen from Figure 21, the radial load acting on the seal results in a CW moment (-ve) about the CCW axis of rotation.

Also, for the seal considered, the centroid due to axial load lies above the CCW rotation axis resulting in a CW moment. The spring forces as well as the seal weight result in a CCW moment about the CCW axis of rotation. Figure 22 shows how these moments (and the net moment) vary with seal pressure differential. During turbine shutdown, seal pressure differential decreases monotonically and as seen in Figure 22, the net moment about the CCW rotation axis is CW (stable configuration) until the pressure differential falls below a threshold, when the net moment turns CCW (unstable configuration). Frictional forces acting at contact points P, G & H generate moments opposing CCW rotation and hence calculations done with the lowest possible friction coefficient will be conservative. If the pressure differential for seal retraction falls below this instability threshold, seal will rotate CCW instead of retracting radially away from the rotor. The seal design must ensure that the DP for seal retraction is always higher than the DP at which seal becomes unstable for CCW rotation or CW rotation.

Figure 23 shows the net moments acting on the seal in its low clearance position for CCW rotation and CW rotation. Note that the instability threshold for CW rotation is lower than that for CCW rotation and hence the seal will rotate CCW if the design is unstable. Also, Figure 23 shows that higher the downstream support hook height, lower the threshold for CCW rotation. Seal design must optimize geometry parameters and spring stiffness to ensure the instability threshold falls significantly below the retraction pressure differential. Seal stability is checked at each point of seal motion during closure and retraction to ensure its stability.

VALIDATION TESTING

To validate the design process and the analytical models predicting the seal closure and retraction behavior, a retractable brush seal segment was fabricated and tested in the laboratory. Figure 24 and Figure 25 show the setup for testing a 10-degree segment of a 1320 mm (52 in) diameter retractable brush seal. Since the primary goal of the testing was to determine seal closure and retraction behavior, rotor surface was simulated and the tests were carried in a static seal test rig. A specially designed housing (shown in Figure 24 and Figure 25) was built with the stator support hooks and the rotor surface to mount the retractable brush seal segment. Custom designed Inconel X-750 leaf springs were used to passively close and retract the seal. Seal pressure drop was changed by controlling airflow through the test rig. Seal closure/retraction was monitored through proximity probes mounted on the housing.

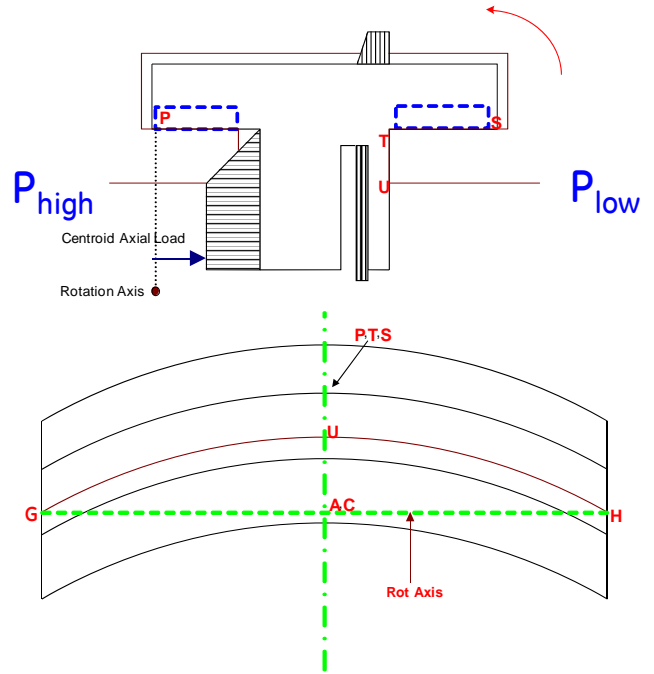


Figure 21 Seal CCW rotation axis under fully closed condition.

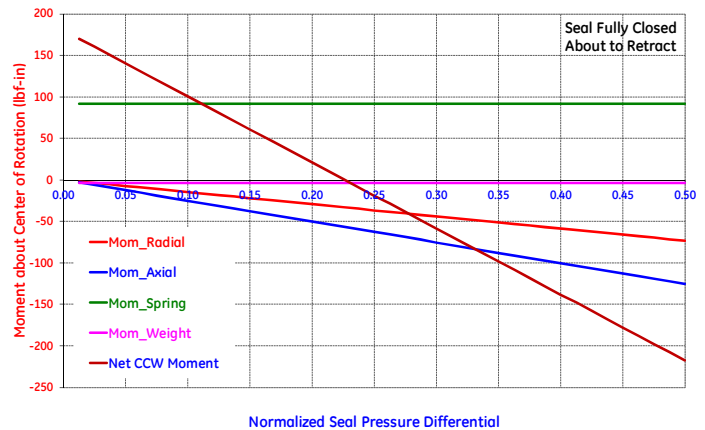


Figure 22 Seal about to retract - Moments due to various forces acting on the seal about the CCW rotation axis.

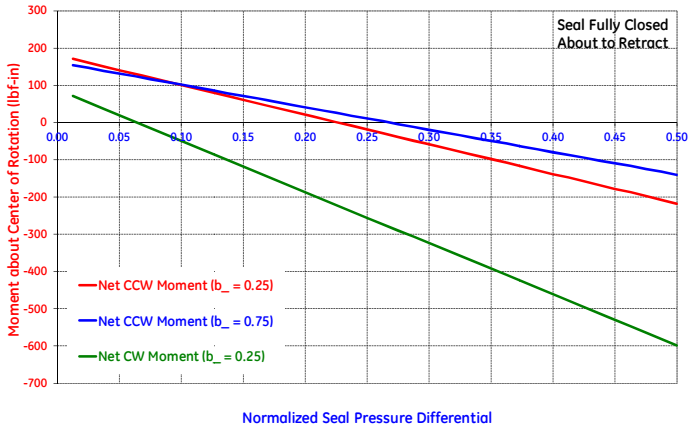


Figure 23 Seal about to retract – Net moments about the CCW and CW rotation axes & the influence of downstream support hook height.

Figure 26 shows the variation of the seal clearance as a function of pressure differential across the seal as it is varied periodically to simulate turbine start up and shutdown processes. During a turbine start up, pressure differential across the seal increases and at a designed point, seal moves from the high clearance position towards the rotor maintaining a tight clearance at the seal operating conditions. During a turbine shutdown, pressure differential across the seal decreases and at a designed point, seal retracts away from the rotor to a high clearance position. Seal motion is found to be very repeatable.

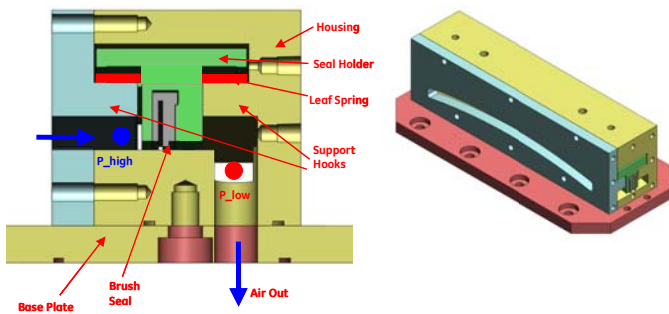


Figure 24 Retractable brush seal test setup.

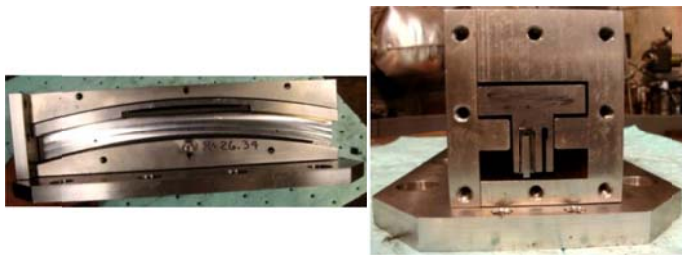


Figure 25 Retractable brush seal test segment and housing - side view (left) and cross section (right).

Figure 27 shows the seal closure curve for three different cycles. At a particular pressure drop, seal sharply moves towards the rotor by a finite distance and then waits for additional pressure increase before making rotor contact. This seal behavior matches with that predicted by the analytical model for $\mu_{static} = 0.3$ and $\mu_{dynamic} = 0.1$.

Figure 28 shows the seal retraction curve for two different cycles. Again at a particular pressure drop, seal retracts sharply away from the rotor by a finite distance reaching its high clearance position. Again this retraction behavior matches with that predicted by the analytical model for $\mu_{static} = 0.3$ and $\mu_{dynamic} = 0.1$.

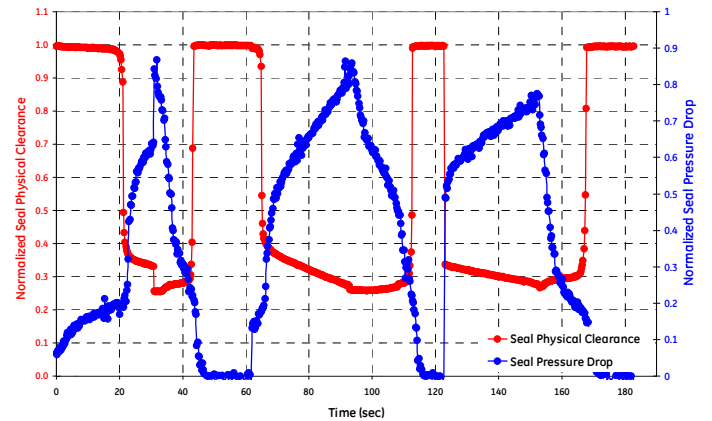


Figure 26 Seal closure and retraction as a function of applied pressure drop simulating start up and shutdown processes.

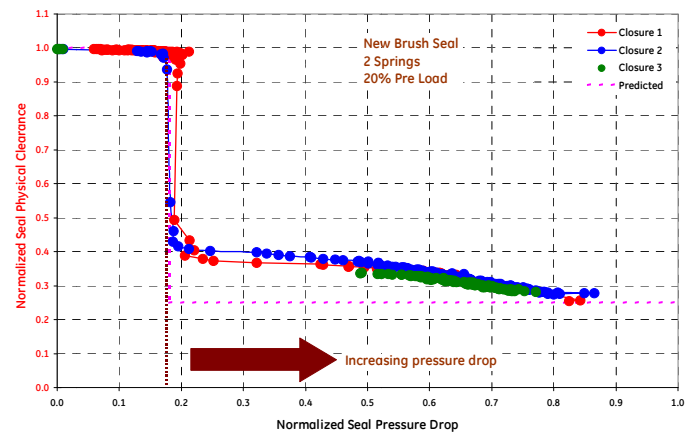


Figure 27 Seal closure behavior – Measured vs Predicted.

Figure 29 shows the seal retraction behavior as recorded by 4 different proximity probes mounted at 4 different locations on the segment as shown. The data clearly indicates that the segment is moving in a purely radial manner and does not tilt or cock about its CW or CCW axis of rotation. Thus stability of seal motion is validated.

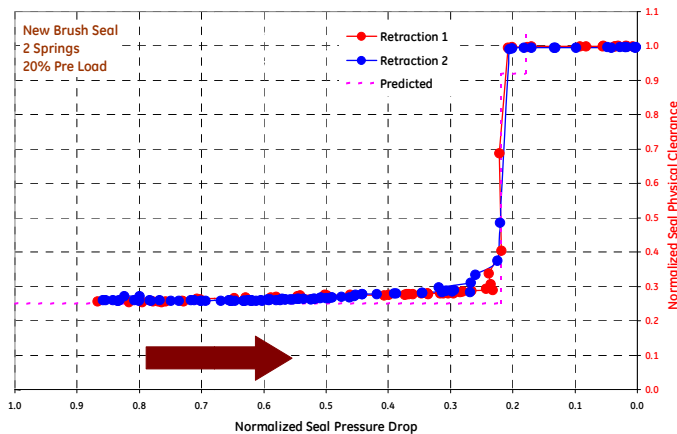


Figure 28 Seal retraction behavior –Measured vs. Predicted.

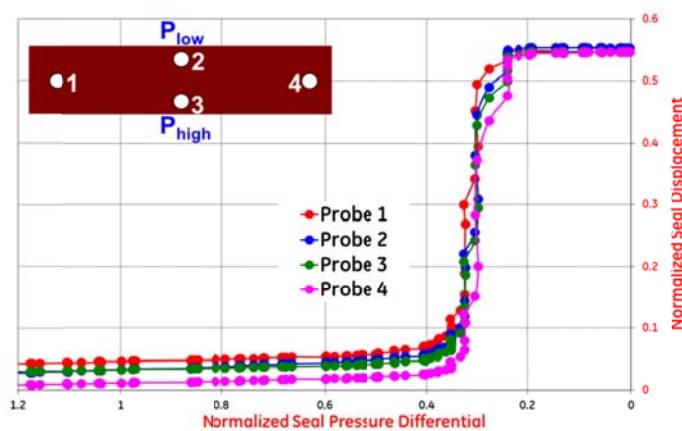


Figure 29 Pure radial motion validating design stability.

SUMMARY

A compressor discharge brush seal can under go significant bristle wear during turbine shut down due to thermally induced interference between the seal and the rotor. To avoid this wear, we proposed mounting it on a retractable seal holder actuated passively by leaf springs. Such a system responds to falling pressure differential across the seal during turbine shutdown causing it to be retracted away from the rotor. Key operational requirements of a retractable brush seal were laid out. Analytical models were developed to predict seal closure and retraction behavior. Key parameters driving the seal motion were identified and their impact on seal motion studied. Seal stability criteria and methodology to check stability of seal motion is presented. An optimal retractable seal segment was designed and a 10-degree segment was tested in the laboratory. The working of a retractable seal was demonstrated and seal design methodology was validated.

ACKNOWLEDGMENT

This work was performed under sponsorship from GE Energy and the US Dept. of Energy under Cooperative Agreement No. DE-FC26-05NT42643.

DISCLAIMER

This paper was prepared as an account of work sponsored by an agency of the United States Government. Neither the United States Government nor any agency thereof, nor any of their employees, makes any warranty, express or implied, or assumes any legal liability or responsibility for the accuracy, completeness, or usefulness of any information, apparatus, product, or process disclosed, or represents that its use would not infringe privately owned rights. Reference herein to any specific commercial product, process, or service by trade name, trademark, manufacturer, or otherwise does not necessarily constitute or imply its endorsement, recommendation, or favoring by the United States Government or any agency thereof. The views and opinions of authors expressed herein do not necessarily state or reflect those of the United States Government or any agency thereof.

REFERENCES

- [1] CE Wolfe, B Fang, O Samudrala, M S Kight, J J Butkiewicz, T McGovern, "Cooling Circuit for Enhancing Turbine Performance," *US20090074589A1*.
- [2] S Dinc, N Turnquist et al. (1998), "Brush Seals in Industrial Gas Turbines—Turbine Section Interstage Sealing," AIAA Paper No. 98-3175.
- [3] BS Bagepalli, MF Aksit, RR Mayer (2001), "Brush seal and rotary machine including such brush seal," *US6257588B1*.
- [4] MF Aksit, RE Chupp, OS Dinc, M Demiroglu (2002), "Advanced Seals for Industrial Turbine Applications: Design Approach and Static Seal Development," *AIAA Journal of Propulsion and Power*, Vol 18, 1254.
- [5] RE Chupp, F Ghasripor, NA Turnquist, M Demiroglu, MF Aksit (2002), "Advanced Seals for Industrial Turbine Applications: Dynamic Seal Development," *AIAA Journal of Propulsion and Power*, Vol 18, 1260.
- [6] S Dinc, M Demiroglu, N Turnquist, J Mortzheim, G Goetze, J Maupin, J Hopkins, C Wolfe, M Florin (2002), "Fundamental Design Issues of Brush Seals for Industrial Applications" *J. Turbomachinery*, Vol 124, 293.
- [7] MF Aksit, JA Tichy (1998), "Wear of Brush Seals: Background and New Modeling Approach," *Tribol. Trans.*, Vol 41, 368.

[8] S Dinc, N Turnquist, R Cromer, G Reluzco, C Wolfe, "Positive biased packing ring brush seal combination," *US6250641*.

[9] C O'Clair, R Chevette, C Greco, J Amirtharajah, "Mounting structure for a packing ring seal segment in a turbine," *US7201560*.

[10] R Chevette, F Baily, "Method and apparatus for variable clearance packing," *US2007274829A1*.

[11] LH Chen, PE Wood, TV Jones, JW Chew (2000), "Detailed experimental studies of flow in large scale brush seal model and a comparison with CFD predictions," *J. Eng. Gas Turbines Power*, Vol 122, Issue 4, 672.

ⁱ Address all correspondence to this author.